



Article

Spatiotemporal Evaluation of Regional Land Use Dynamics and Its Potential Ecosystem Impact under Carbon Neutral Pathways in the Guangdong–Hong Kong–Macao Greater Bay Area

Haoming Chen ¹, Na Dong ^{1,2,*}, Xun Liang ³ and Huabing Huang ^{1,2}

¹ School of Geospatial Engineering and Science, Sun Yat-sen University, Zhuhai 519082, China; chenhm85@mail2.sysu.edu.cn (H.C.); huanghb55@mail.sysu.edu.cn (H.H.)

² Key Laboratory of Natural Resources Monitoring in Tropical and Subtropical Area of South China, Ministry of Natural Resources, Zhuhai 519082, China

³ School of Geography and Information Engineering, China University of Geosciences, Wuhan 430078, China; liangxun@cug.edu.cn

* Correspondence: dongn6@mail.sysu.edu.cn; Tel.: +86-15875653616

Abstract: The spatiotemporal distribution of ecosystem service values (ESVs) and ecological risk are critical indicators to represent the regional ecological protection level and potential of sustainable development, which largely depend on land-use patterns. Aiming to contribute to global climate mitigation, China has proposed dual-carbon goals that would remarkably influence the land-use/cover change (LUCC) distribution. Based on the Landsat land cover data of 2000, 2010 and 2020 and multi-source satellite products, several driving factors are integrated into the patch-generating land use simulation (PLUS) model to simulate future LUCC patterns for the Guangdong–Hong Kong–Macao Greater Bay Area (GBA) under rapid urbanization, cropland protection and carbon neutral (CN) scenarios from 2020 to 2050. Spatial–temporal ecosystem service and ESVs are allocated using IN-VEST and the equivalent factor method and thus ecological risks are evaluated using the entropy method. Results indicate that forest growth is the largest under the CN scenario, especially in the northwestern and northeastern GBA, exceeding 25,800 km² in 2050, which results in both the highest habitat quality and carbon storage. The largest ESVs, reaching higher than 5210 yuan/pixel, are found in the CN scenario, particularly expanding toward the suburban area, leading to the lowest ecological risks. From 2020 to 2050, habitat quality, carbon storage and ESVs improve, while ecological risks decline in the CN scenario. This research provides implications for economic and ecological balanced development and gives references to the carbon-neutral pathway for the GBA.

Keywords: land use pattern; scenario simulation; ecosystem services; carbon neutral; spatial aggregation



Citation: Chen, H.; Dong, N.; Liang, X.; Huang, H. Spatiotemporal Evaluation of Regional Land Use Dynamics and Its Potential Ecosystem Impact under Carbon Neutral Pathways in the Guangdong–Hong Kong–Macao Greater Bay Area.

Remote Sens. **2023**, *15*, 5749.

<https://doi.org/10.3390/rs15245749>

Academic Editors: Guangdong Li, Sanwei He and Zhiqi Yang

Received: 23 October 2023

Revised: 10 December 2023

Accepted: 12 December 2023

Published: 15 December 2023



Copyright: © 2023 by the authors. Licensee MDPI, Basel, Switzerland. This article is an open access article distributed under the terms and conditions of the Creative Commons Attribution (CC BY) license (<https://creativecommons.org/licenses/by/4.0/>).

1. Introduction

Ecosystem services (ES), connecting the natural environment with human society, make continuous contributions to human welfare, which largely depends on land use/cover change (LUCC) and the corresponding strategies. In recent decades, China proposed reform and opening up, which means that international trade and development opportunities have largely increased. It leads to rapid economic growth and dramatic LUCC, resulting in severe degradation of the ES quality. In recent years, China proposed a dual-carbon strategy to control carbon emissions, finally achieving sustainable development, which would potentially affect the ES evolution. To quantitatively measure ES changes, ecosystem service value (ESV) changes and the accompanying ecological risk assessment comprehensively reflect the ecosystem function and potential threat to the ecosystem. Therefore, the evaluation of future LUCC-induced ESV changes and the exposed ecological risks under multiple socio-economic and ecological pathways, giving a glimpse into reasonable decision making on land-use management and ecological protection, deserve special attention.

In order to gain a better understanding of the potential impact of future policies on the spatiotemporal distribution of LUCC, a series of scenarios are designed and combined with the future LUCC [1]. Zhang et al. [2] and Schirpke et al. [3] proposed four scenarios to simulate LUCC, concerning different development patterns such as cropland protection, forest protection, rapid urbanization and so on. In contrast to earlier scenarios, the carbon neutrality scenario prioritizes the enhancement of carbon storage capacity and the achievement of sustainable development goals, imposing strict limitations on urban expansion. How different scenarios would stimulate multiple land-use conversions still needs to be investigated. A variety of LUCC models have been developed in recent decades, such as CLUE-S model [4] and FORE-SCE model [5]. Liang et al. [6] proposed a patch-generating land use simulation (PLUS) model, which uses a multi-type patch generation strategy and models the simultaneous evolution of land-use patches and has been widely applied in the LUCC simulations. Gao et al. [7] applied the PLUS to simulate the LUCC of Nanjing in 2025 under four scenarios; Li et al. [8] used the PLUS to simulate the Sichuan–Yunnan ecological barrier in 2026 under three scenarios. Therefore, the PLUS model, an approach that combines a CA model with a patch-generating simulation strategy, is a suitable tool for investigating the interactive relationship between policies and land-use patterns.

To quantitatively evaluate ecosystem changes induced by LUCC, the Integrated Valuation of Ecosystem Services and Tradeoffs (INVEST) model is widely used in the assessment of ES changes, which contains nine terrestrial modules and eight marine modules, including carbon storage and sequestration, crop production, habitat quality, nutrient delivery ratio and so on [9–16]. It uses land-use data and related economic and biophysical data to predict the relevant ES under multiple scenarios. In recent years, ES has been further classified into three top categories by the European Environment Agency (EEA)—provisioning, regulating and maintenance, and cultural services [17]—which can be quantitatively evaluated by ESV changes, which assign values to the ES based on LUCC and indicate the ecological sustainable capability [18]. To calculate ESVs, Costanza et al. [19] proposed a global ecosystem service equivalent factor table. Then, Xie et al. [20] evaluated the ecological assets of the Tibetan Plateau according to the ecosystem service value per unit area based on the Chinese terrestrial ecosystem. Xie et al. [21] improved the equivalent coefficients table for ESVs per unit area of China, which has been widely used to calculate ESVs [18,22–24]. Related research is shown in Table 1. However, the impacts of LUCC on ES, ESV and their induced ecological risks are rarely considered together in previous studies. We provide a comprehensive evaluation of the impacts of LUCC on various ecological indicators. In our research, the differences of ES and ESV among three scenarios deserve special attention.

Table 1. Studies related to land-use simulation and ecological service and risk assessment.

Research	Land Use Change Scenario	Region	Ecological Service Value Assessment	Ecological Risk Assessment
Hu et al. [18]	Historical	the Pearl River Delta (PRD)	the equivalent coefficients table method	
Liu et al. [22]	Historical	the PRD		
Schirpke et al. [3]	Business as usual scenario, 'Liberalization' scenario, 'Rewilding' scenario, 'Food sovereignty' scenario	South Tyrol, Italy	derived from the ES supply, and was weighted by the socio-cultural preference values	/
Jiang et al. [25]	SSP1, SSP2, SSP3, SSP4, SSP5	Zhengzhou	eco-environmental quality index, ecological contribution rate of land use transition	

Table 1. Cont.

Research	Land Use Change Scenario	Region	Ecological Service Value Assessment	Ecological Risk Assessment
Peng et al. [26]	Natural increase scenario, economic development scenario, ecological protection scenario	Wuhan	the equivalent coefficients table method	/
Zhang et al. [2]	Natural development scenario, cultivated land protection scenario, ecological protection scenario, urban development scenario	Wuhan		
Jin et al. [27]	Historical	Delingha city		land use types, the loss index of each land use type
Xu et al. [28]	Natural growth scenario, ecological protection scenario	Xinjiang	/	landscape loss index, ecological sensitivity index
Zhang et al. [29]	SSP1, SSP2, SSP3, SSP4, SSP5	Fujian Delta region		landscape disturbance index, the landscape vulnerability index, and land use types
Gao et al. [7]	BAU scenario, RED scenario (maximum economic benefit), ELP scenario (maximize the ecological benefit)	Nanjing	the equivalent coefficients table method	urban expansion pressure, landscape ecological risk, grain reserve pressure, ecological degradation pressure

Ecological risk serves as an indicator to reflect the negative impacts of human activities on the ecological environment [30,31]. In previous studies, ecological risk is usually evaluated in two ways: based on risk sources and sinks [32–34] or on landscape patterns [29,35]. The method using risk sources contains three steps, including risk source identification, receptor analysis, and evaluation of exposure and damage [36]. However, this method may not comprehensively consider various risk sources, making it unsuitable for assessing local ecological risks. Conversely, the method based on landscape patterns, which constructs a risk assessment model according to the risk of each land patch, is more precise. The ecological risk index (ERI), widely used to evaluate regional ecological risk, can quantitatively evaluate ecological risk based on the land use type of each patch [27,37–39]. It establishes a more intricate correlation between LUCC and ecological risk. However, it solely takes into account the quantitative change of land use areas, without considering the ecological aspects of LUCC, leading to an incomplete evaluation outcome. To address this limitation, Gao et al. [7] incorporated the entropy method and ecological indicators, such as ESVs and ecological capability (EC), into the ecological risk assessment model to comprehensively evaluate the ecological effects on ecological risk. It has transitioned from a simplistic evaluation of ecological risk based solely on the quantitative characteristics of land use types to a comprehensive analysis that considers various factors, including ESVs and EC. Some researchers use the Geodetector model to evaluate the spatial pattern of NDVI and LAI [40,41], which is a reference to the evaluation of ecological risk.

In this paper, several problems need to be solved. Firstly, aiming to evaluate the impacts of land-use policies on the future LUCC, three scenarios, including cropland protection (CP) scenario, rapid urbanization (RU) scenario and carbon neutral (CN) scenario,

are proposed to simulate different development patterns. Based on the historical land-use data and driving factors, LUCC from 2030 to 2050 under three scenarios are simulated. Secondly, in order to evaluate the spatiotemporal influence of LUCC on the ecological system, both the equivalent coefficients method and the INVEST model are applied to evaluate carbon storage, habitat quality changes and ESVs referring to future scenarios. Thirdly, the ecological risk among three scenarios in the future is assessed and the ecological risk maps are generated. Finally, the generation of scientific suggestions and effective support is expected to promote the sustainable development of the GBA region.

2. Materials and Methods

2.1. Study Area

The GBA, located in the middle of Guangdong Province, is a mega-urban agglomeration over Southern China, spanning from 111.5°E to 115.5°E and 21.5°N to 25°N (Figure 1). The GBA falls under the subtropical monsoon climate zone, with a mean annual rainfall of 1600–2000 mm. The region's vegetation primarily comprises subtropical evergreen broadleaf forests. The GBA, an extensive area of 54,574 km², is composed of Guangzhou, Shenzhen, Huizhou, Zhuhai, Foshan, Dongguan, Jiangmen, Zhongshan, Zhaoqing and the Hong Kong and Macau special administrative regions. After the reform and opening-up of the 1980s, the GBA has undergone rapid economic development, thus causing urban extension, land cover changes and large uncertainty in the ecological system evolution. With the increasing densely distributed population and ecological land occupation, the GBA gains great pressure on its cropland redline retention and forest protection which is closely related to the land management pathways and the ecological policies. Therefore, the GBA is a typical representative that reflects LUCC and the induced ecological environment change in China.

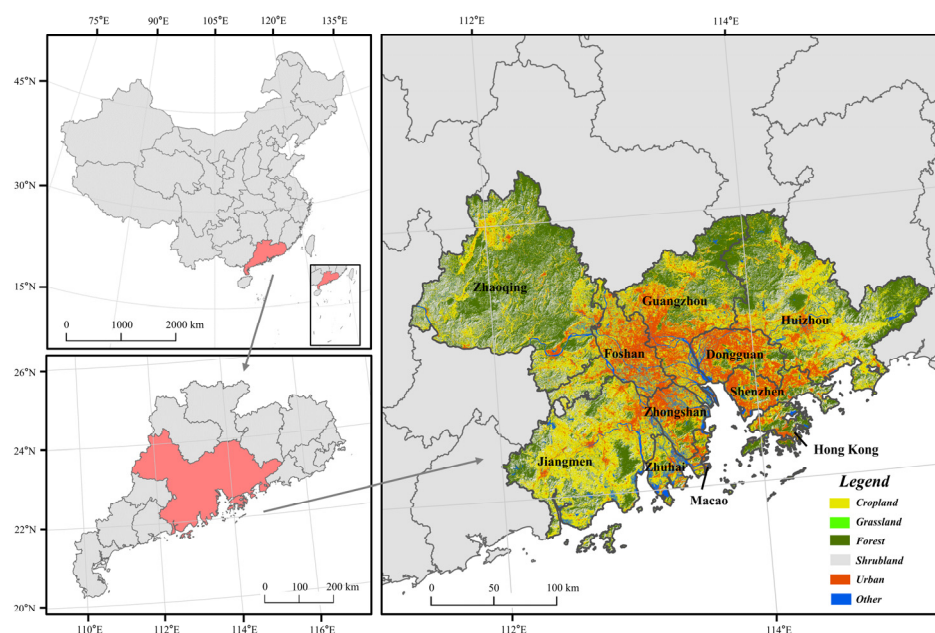


Figure 1. General location of Guangdong–Hong Kong–Macao Greater Bay Area.

2.2. Data Sources

2.2.1. Land-Use Data and Driving Factors

Land-use data for the years 2000, 2010 and 2020, at a resolution of 30 m, are obtained from the Chinese Academy of Sciences and harmonized into 6 basic land use types (cropland, grassland, forest, shrubland, urban and other) [42]. The product is produced by combining a time series of Landsat imagery (Landsat-TM/ETM/OLI) and high-quality training data from the Global Spatial Temporal Spectra Library on the Google Earth Engine

computing platform. Both evergreen broadleaved forests and deciduous broadleaved forests with different traits are merged into forests. All types of shrubland, including evergreen shrubland, deciduous shrubland and sparse shrubland, are classified as shrubland. Rainfed cropland and herbaceous cover are considered to be cropland and grassland, respectively. Impervious surfaces are regarded as urban areas. Wetlands, water bodies, permanent ice and snow are merged into the “other” category (Table S1). Nine driving factors are adopted in the PLUS model, which includes climatic data (precipitation, temperature, vapor pressure deficit and solar radiation), socioeconomic data (GDP, population), DEM data, road network, river, railway data and soil type (Table S2, Figure S2). These driving factors data are all resampled to new data with a resolution of 30 m by ArcGIS.

2.2.2. Statistical Data

Statistical data are used in the calculation of ES and ESVs. The INVEST model used in the ES evaluation requires carbon pool data and threat sources data to evaluate carbon storage and habitat quality respectively. The carbon pool data is proposed by Wu et al. [43] and the threat sources data is from Terrado et al. [44]. In order to calculate the standard unit equivalent factor for the ESVs, the production values of both the early indica rice and the late indica rice are obtained from the national compilation of agricultural cost-benefit information and the sown area data is obtained from the *Guangdong Statistical Yearbook of 2020* (<http://tjnj.gdstats.gov.cn:8080/tjnj/2021/directory/11/html/11-13.htm>, accessed on 1 January 2021).

2.3. Methodology

In this research, the changes of future ESVs and ecological risks are evaluated for the GBA region based on LUCC under three scenarios (cropland protection, rapid urbanization and carbon neutral pathways) using the PLUS model, the INVEST, the equivalent coefficient method and the entropy method. The flowchart is shown in Figure 2.

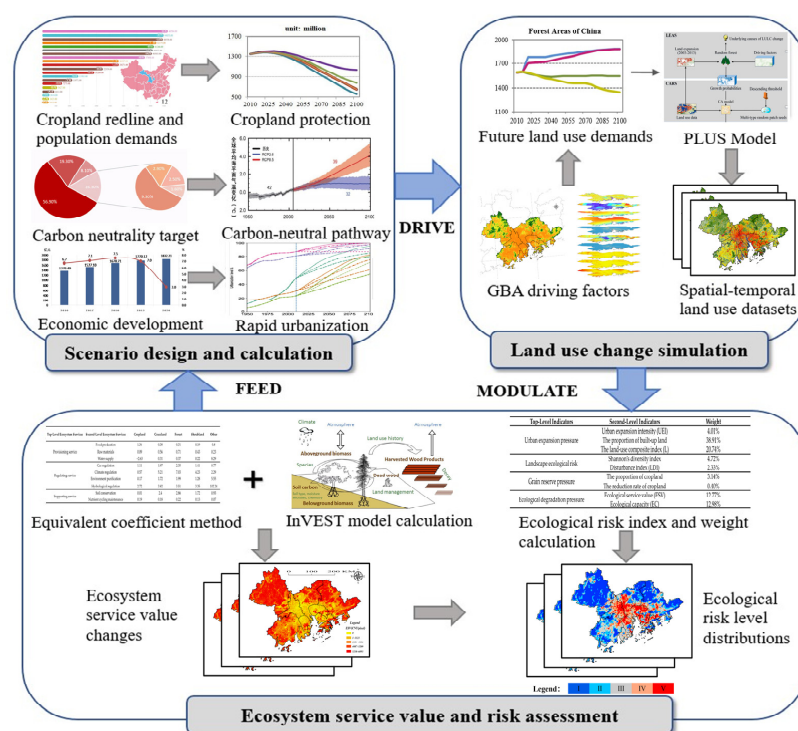


Figure 2. The framework for assessing land use dynamics and the ecosystem impacts under multi-scenarios.

2.3.1. Land Use Change Scenario

Cropland protection (CP) scenario: The goal of the CP scenario is to prevent the encroachment of other land use types on cropland. With reference to The National Territorial Plan 2016–2030, China set the target that the retention area of cropland is 1.865 billion mu in 2020 and 1.825 billion mu in 2030. Based on this, the changing rate of cropland is calculated and applied to evaluate the cropland demands between 2030 and 2050. Accordingly, the changing rates for grassland, forest and shrubland are controlled based on their areas in 2020. Conversions between cropland, forest and shrubland are allowed while urban expansion is restricted. No changes are made to the area of “other” land use type.

Rapid urbanization (RU) scenario: The RU scenario prioritizes urban expansion regardless of its impact on ecology. During the period of 2010–2020, the rapid economic development has led to a substantial rate of urban expansion. Based on this, the speed of urban expansion from 2010 to 2020 is utilized to estimate urban area changes from 2030 to 2050. The probability of conversion from cropland, forest and shrubland to urban increases while the changing rates of cropland, forest, grassland and shrubland are controlled based on their respective areas in 2020. The area of “other” remains unchanged.

Carbon neutral (CN) scenario: The carbon neutral scenario aims to maximize carbon storage and sequestration while ensuring food security. The area of forest in China will increase by 47 million hectares from 2020 to 2050 [45]. Based on the proportional area of forest in the GBA compared to the national forest area in 2020 and its growth rate, forest demands in the GBA between 2030 and 2050 are evaluated. While the preservation of cropland is a priority, the conversions from shrubland and grassland to forest are controlled based on the current area of grassland and shrubland in 2020. To achieve the desired outcome, the total area of forest, shrubland and grassland in 2050 will be equal to their combined total in 2020. The area of “other” land use type remains unchanged.

2.3.2. Land Use Change Simulation

In order to promote high-resolution dynamic simulation of LUCC, a patch-generating land-use simulation model (PLUS model) proposed by Liang et al. [6] is adopted to explore the relationships between LUCC and different driving factors. Based on a land expansion analysis strategy (LEAS), this model proposes a rule mining framework to obtain the development potential of different land use types. Following the LEAS part, land-use expansion of two years is first extracted and sampling points are randomly selected according to the types of the land-use expansion. Random Forest Classification (RFC) algorithms are then used to calculate the relationship between driving factors and the growth of each land use type. The relationship between the land use conversions and nine driving factors is analyzed. Finally, a cellular automata (CA) model with a patch-generating simulation strategy is used to simulate future land-use patterns.

2.3.3. Ecosystem Service Assessment

Ecosystem service changes are assessed based on the future LUCC (2030, 2040, 2050) pattern under multiple scenarios using the INVEST 3.12.0 model [46,47]. Two typical kinds of ES, including carbon storage and habitat quality, are selected to evaluate their responses to LUCC driven by different policies and measures. The Carbon Storage and Sequestration module of the INVEST model is used to evaluate the regional amount of carbon storage and carbon sequestration. Carbon storage is derived from four carbon pools: aboveground biomass, belowground biomass, soil and dead organic matter. Since the dead organic contains a small amount of carbon, we only consider the sum of aboveground biomass, belowground biomass and soil as the total carbon storage. The habitat quality is also calculated by the INVEST, which requires the LUCC map, threats table, sensitivity table and a half-saturation constant. The threats table and sensitivity table are adopted from

Terrado et al. [44]. The half-saturation constant is set as 0.5 by default while the habitat quality is calculated by the following formula:

$$Q_{xj} = H_j \times \left(1 - \left(\frac{D_{xj}^z}{D_{xj}^z + k^z} \right) \right) \quad (1)$$

where Q_{xj} represents the habitat quality in grid cell x with j th land use type; H_j represents the habitat score assigned to j th land use type, which ranges from 0 to 1. The higher the habitat score, the better the habitat quality.

2.3.4. Ecosystem Service Value Calculation

Based on the LUCC, we use a new dynamic equivalent factor table proposed by Xie et al. [21] to calculate ESVs, which is shown in Table 2. The standard unit equivalent factor refers to the economic value of the annual average natural grain yield per hectare of cropland, which indicates the early indica rice and the late indica rice in GBA. According to the method of Xie et al. [48], the net profit of crop production per unit area of cropland ecosystem is used as the standard unit equivalent factor. However, the net profit data is difficult to obtain and we use one seventh of the grain production value [20] instead. In addition, the proportion of sown area for grain crops is also considered. The formula is as follows:

$$D = \frac{1}{7} \times (S_e \times F_e + S_l \times F_l) \quad (2)$$

where D represents the standard unit equivalent factor (yuan/mu). S_e and S_l represent the percentage of sown area of the early indica rice and the late indica rice in the total sown area of rice, respectively. F_e and F_l represent the production values of the early indica rice and the late indica rice (CNY/mu), respectively. According to the national compilation of agricultural cost–benefit information, the production values of the early indica rice and the late indica rice in 2020 were 1214.74 CNY/mu and 1372.81 CNY/mu, respectively, while the sown area of the early indica rice and the late indica rice in 2020 are 1303.7 mu and 1447.95 mu, respectively. Based on the formula, the standard unit equivalent factor is calculated as 185.42 CNY/mu or 2781.25 CNY/ha.

Table 2. The equivalent coefficients for ESVs per unit area.

Top-Level Ecosystem Services	Second-Level Ecosystem Services	Cropland	Grassland	Forest	Shrubland	Other
Provisioning service	Food production	1.36	0.38	0.31	0.19	0.8
	Raw materials	0.09	0.56	0.71	0.43	0.23
	Water supply	−2.63	0.31	0.37	0.22	8.29
Regulating service	Gas regulation	1.11	1.97	2.35	1.41	0.77
	Climate regulation	0.57	5.21	7.03	4.23	2.29
	Environment purification	0.17	1.72	1.99	1.28	5.55
	Hydrological regulation	2.72	3.82	3.51	3.35	102.24
Supporting service	Soil conservation	0.01	2.4	2.86	1.72	0.93
	Nutrient cycling maintenance	0.19	0.18	0.22	0.13	0.07

Urban type is unbeneficial for ecosystem service development and the value is 0 for each ecosystem service type.

Based on the equivalent factor table, the ecosystem service value can be calculated as follows:

$$ESV_{ij} = VC_{ij} \times A_i \times D \quad (3)$$

where ESV_{ij} represents the ecosystem service value of ecosystem service function type j in land use type i . VC_{ij} represents the value coefficient for ecosystem service function type j of land use type i . A_i represents the area of land use type i . Additionally, the relationship between LUCC and ESVs is revealed using the circular migration flow analysis approach

first [49,50]. Exploratory spatial data analysis is also adopted to investigate the spatial distribution patterns and heterogeneity characteristics of ESVs in the study area [51,52]. We utilize ArcGIS10.8 and GeoDa1.18 to calculate Getis-Ord G_i^* to identify high- and low-value aggregation areas of ESVs and determine the local state of cold and hot spots in spatial ESVs changes under different scenarios.

2.3.5. Ecological Risk Assessment

Based on the risk assessment method of Gao et al. [7], nine indicators are selected to evaluate the ecological risk, reflecting impact aspects from urban expansion pressure, landscape ecological risk, grain reserve pressure and ecological degradation pressure, respectively, which include several second-level indicators (Table 3). The urban expansion intensity (UEI) is calculated using the specific time interval and the proportion of the changing urban area over the specific time interval to the initial area of the urban area. The land-use composite index (L) represents the extent of human development on land, which quantifies the impact of human activities on the land by grading each land use type. The disturbance index (LDI) is comprehensively determined by the patch density, the splitting index and the landscape division index. Their weights are given based on the method of Han et al. [53]. The calculation is realized using the software Fragstats 4.2. ESVs from the previous part are applied in the calculation of the ecological capability (EC). The formula is as below:

$$EC = \sum_{i=1}^6 a_i \times r_i \times y_i \quad (4)$$

$$r_i = \frac{P_i}{\bar{P}_{NP}} \quad (5)$$

$$y_i = \frac{P_i}{\bar{E}_i} \quad (6)$$

where a_i is the area of i th LUCC. r_i is the equilibrium factor. y_i is the production factor. P_i is the ESV per unit area of i th land use type. \bar{P}_{NP} is the average ESV per unit area of all land use types. \bar{E}_i is the national average ESV per unit area of i th land use type [54].

Table 3. The indicators of ecological risk and their weights.

Top-Level Indicators	Second-Level Indicators	Weight
Urban expansion pressure	Urban expansion intensity (UEI)	4.01%
	The proportion of built-up land	38.91%
	The land-use composite index (L)	20.74%
Landscape ecological risk	Shannon's diversity index	4.72%
	Disturbance index (LDI)	2.33%
Grain reserve pressure	The proportion of cropland	3.14%
	The reduction rate of cropland	0.40%
Ecological degradation pressure	Ecosystem service value (ESV)	12.77%
	Ecological capacity (EC)	12.98%

The entropy method is used to evaluate the weight of each indicator [55], which is based on that the smaller the entropy value, the greater the degree of dispersion of the index, and the greater the influence of the index on the comprehensive evaluation, thus giving a greater weight. We initially established a 3 km × 3 km fishing net, dividing the GBA into 2590 sample units. Subsequently, we calculate the number and area of patches for each land use type within each sample unit. Based on this, the values of nine indicators within each sample unit are computed, and the weights of these indicators can be obtained by the entropy method and standardization is performed according to their positively or negatively impact direction. These indicators and their weights are shown in Table 3.

3. Results

3.1. Land Use Demands under Future Scenarios

The different scenarios and pathways result in diverse land use demands (Figure 3). In the RU scenario, the rapid urban expansion is the primary objective, resulting in a high urban growth rate reaching 0.8. The urban is mainly transformed from cropland and forest, which leads to a significant reduction of these two land use types. The rate of forest loss is approaching 0.4. By contrast, the CP scenario attaches more importance to cropland protection, resulting in a slower rate of cropland reduction. The CN scenario aims to enhance regional carbon storage capacity, improve the ecological environment and ensure food security. In this scenario, cropland and forest are well preserved, and the area of cropland decreases at the same pace as the CP scenario. At the same time, the forest increases significantly, with a growth rate of 0.38. According to our prediction, the area of forest will exceed 24,500 km² in 2050, with the large increase primarily coming from shrubland. As a result, the shrubland experiences an extremely significant decrease in the CN scenario, with an area substantially less than that in the CP and RU scenarios. In order to reduce the impact of urban expansion, the CN scenario imposes strict restrictions on urban expansion, with an expansion rate of approximately 0.2. The urban area will be less than 10,000 km² by 2050, which is far less than that in the CP and RU scenarios.

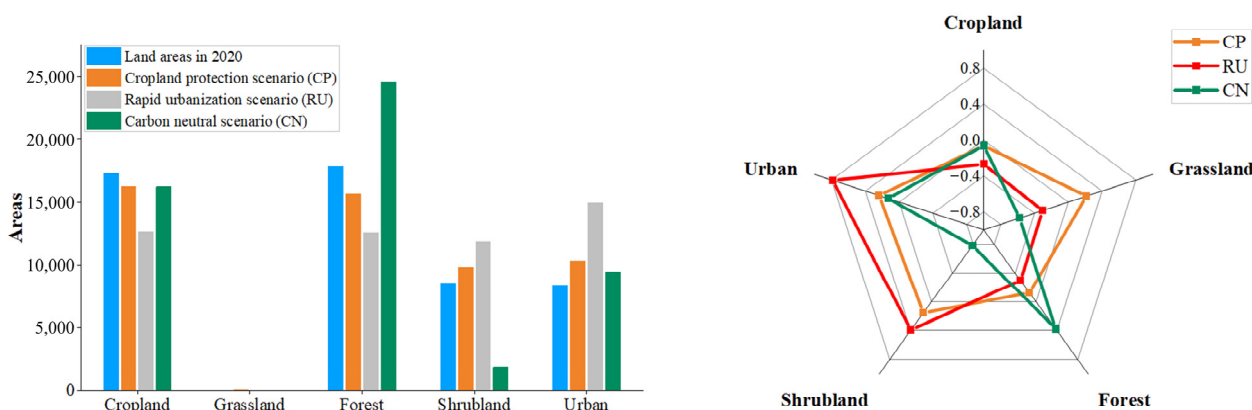


Figure 3. Left: Comparison of land use demands between 2020 and 2050 under three future scenarios. The blue columns are land use areas in 2020, orange columns are for 2050 cropland protection (CP) scenario, grey columns are for 2050 rapid urbanization (RU) scenario and green columns are for 2050 carbon neutral (CN) scenario. Right: net change rate of 2050 compared with land use areas of 2020 under three scenarios.

3.2. Land Use Change Simulation

Validation for historical LUCC simulation is evaluated using 2000 and 2010 land-use datasets and the distribution is shown in Figure S1. The kappa coefficient is 0.80 and the overall simulation accuracy is 0.86, indicating that the PLUS model is effective for capturing spatial landscape changes. Results of the simulation in 2030, 2040 and 2050 under three scenarios (CP, RU and CN) are simulated based on the 2020 land-use data which is shown in Figure 4 and Table 4. Spatial pattern evolution under three future scenarios demonstrates distinct characteristics as they prioritize different environmental control targets. In the RU scenario, cropland and forest are heavily encroached by urban expansion along the boundaries of the urban and rural areas from 2030 to 2050, which leads to significant anthropogenic interference on the ecological system. In the CP scenario, cropland is well preserved with most distributed in southwestern and southeastern GBA. The urban expansion in the CP scenario is slower than that in the RU scenario. In the CN scenario, the forest is expanding, especially to the northwestern and northeastern GBA, at the cost of shrubland. Cropland is also well preserved to the same degree as the CP scenario. The CN scenario shows the most evident changes in both type and total area of vegetation.

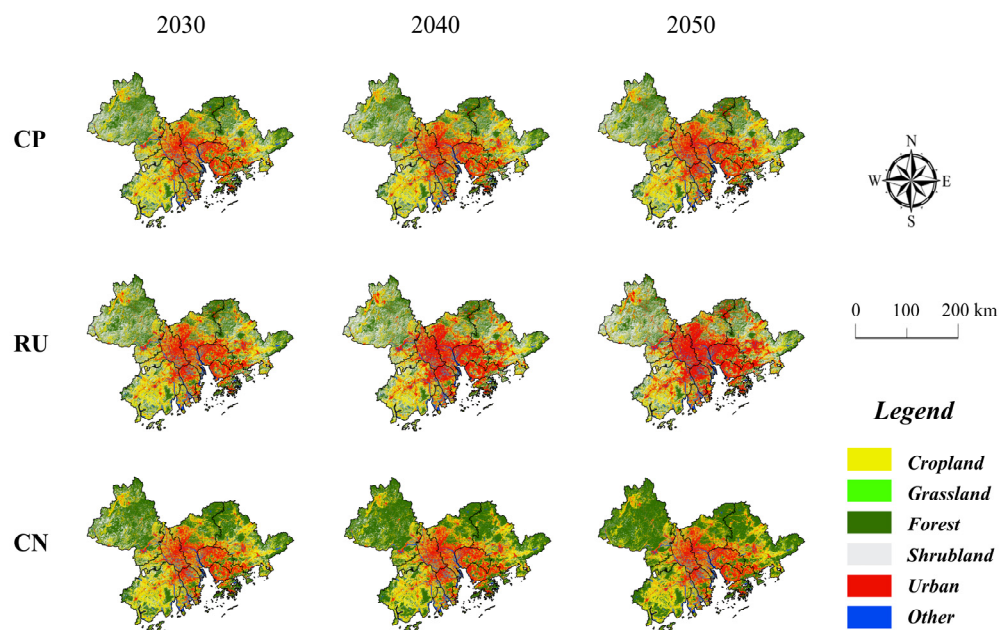


Figure 4. Dynamic landscape patterns for 2030, 2040 and 2050 under multi-scenarios. Note: CP, RU and CN refer to the cropland protection scenario, rapid urbanization scenario and carbon neutral scenario, respectively.

Table 4. The percentage of each land use type for 2020, 2030, 2040 and 2050 under multi-scenarios.

Scenario	Year	Cropland	Grassland	Forest	Shrubland	Urban	Other
/	2020	31.247%	0.011%	32.228%	15.395%	15.110%	6.008%
CP	2030	30.577%	0.011%	30.725%	16.802%	15.878%	6.008%
	2040	29.921%	0.012%	29.244%	17.667%	17.149%	6.008%
	2050	29.279%	0.013%	28.228%	17.766%	18.704%	6.008%
	RU	2030	28.695%	0.012%	28.793%	17.819%	18.673%
RU	2040	25.928%	0.011%	25.161%	19.814%	23.077%	6.008%
	2050	22.832%	0.008%	22.712%	21.447%	26.994%	6.008%
CN	2030	30.577%	0.008%	37.009%	10.632%	15.766%	6.008%
	2040	29.921%	0.006%	41.789%	5.855%	16.422%	6.008%
	2050	29.279%	0.005%	44.313%	3.317%	17.078%	6.008%

3.3. Spatial–Temporal Changes of Ecosystem Service

3.3.1. Carbon Storage

Carbon storage changes are dependent on land-use patterns and exhibit significant variations among three scenarios (Figure 5, Table 5). In the RU scenario, areas with high carbon storage capacity are located in the northwestern and northeastern GBA, particularly in Zhaoqing and Huizhou, whereas the central GBA, with a high economic level and dense urbanization, shows low carbon storage capacity. The carbon storage capacity declines from 2030 to 2050 due to the reduction of both cropland and forest. It is worth noting that the carbon storage in the central GBA is declining rapidly, showing an extensive decreasing trend to the outward. The spatiotemporal distribution and growing trend of carbon storage changes in the CP scenario are similar to those in the RU scenario. However, the total carbon storage capacity of GBA in the CP scenario is higher than that in the RU scenario. The CN scenario exhibits the most abundant carbon storage capacity among the three scenarios as forest areas are the biggest under this scenario. The carbon storage capacity of northwestern and northeastern GBA is relatively large, especially in rural areas (e.g., northwestern and northeastern regions). In contrast to the CP and RU scenarios, the total carbon storage capacity demonstrates a significant increasing trend from 2030 to 2050

in the CN scenario. Generally, carbon storage distributions are lower in the middle but higher in the surrounding regions among the three scenarios.

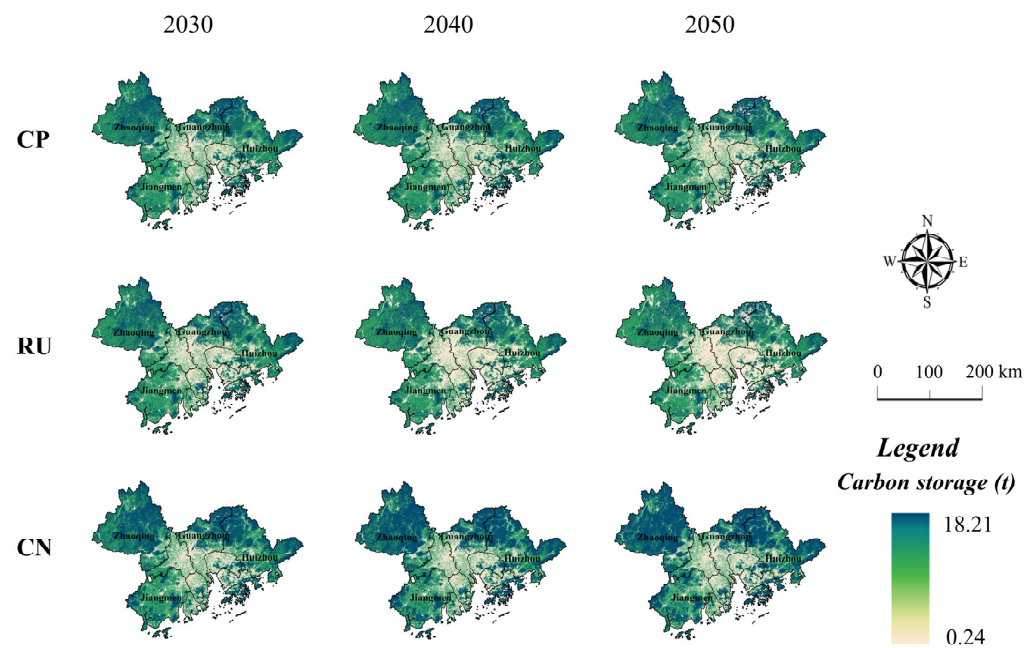


Figure 5. Dynamic carbon storage distributions for 2030, 2040 and 2050 under multi-scenarios (unit: ton). Note: CP, RU and CN refer to the cropland protection scenario, rapid urbanization scenario and carbon neutral scenario, respectively. Cities with higher carbon storage in GBA are marked.

Table 5. Carbon storage for 2030, 2040 and 2050 under multi-scenarios (unit: ton).

Scenario	Year	Cropland	Grassland	Forest	Shrubland	Urban	Other
/	2020	202,038,233	94,873	287,357,803	87,725,762	1,742,112	3,823,298
	2030	197,704,969	93,458	273,953,927	95,739,005	1,830,582	3,823,298
	2040	193,464,649	98,753	260,748,807	100,667,960	1,977,139	3,823,298
	2050	189,315,280	115,197	251,693,685	101,235,551	2,156,509	3,823,298
RU	2030	185,535,153	99,137	256,733,535	101,534,104	2,152,920	3,823,298
	2040	167,643,701	98,124	224,349,632	112,906,215	2,660,603	3,823,298
	2050	147,628,789	66,039	202,505,588	122,206,343	3,112,205	3,823,298
CN	2030	197,704,890	65,445	329,986,965	60,583,983	1,817,733	3,823,298
	2040	193,464,570	48,092	372,603,634	33,360,121	1,893,355	3,823,298
	2050	189,315,280	40,298	395,114,261	18,898,717	1,968,977	3,823,298

3.3.2. Habitat Quality

Similar to carbon storage, the habitat quality which reflects the sustainability of the ecosystem environment is also closely related to scenarios and landscapes (Figure 6). In the RU scenario, the habitat quality declines rapidly due to urban expansion, especially in the central GBA, including Guangzhou, Shenzhen, Foshan, Dongguan and Zhongshan. The decline is gradually spreading from the middle to the periphery from 2030 to 2050. The northwestern, southwestern and northeastern GBA show relatively lower declines from 2030 to 2050, as those suburban areas are far from urban areas. In contrast, the habitat quality in the CP scenario is slightly higher than that in the RU scenario, declining in the central GBA but improving slightly in the surrounding regions. The CN scenario has the highest habitat quality, with extensive improvements in the northwestern, southwestern and northeastern GBA as a result of increasing forest areas. The habitat quality in the central GBA will remain steady from 2030 to 2050. Overall, the three scenarios exhibit

similar patterns of habitat quality distributions with lower quality in the central GBA and higher quality extended in the surrounding areas.

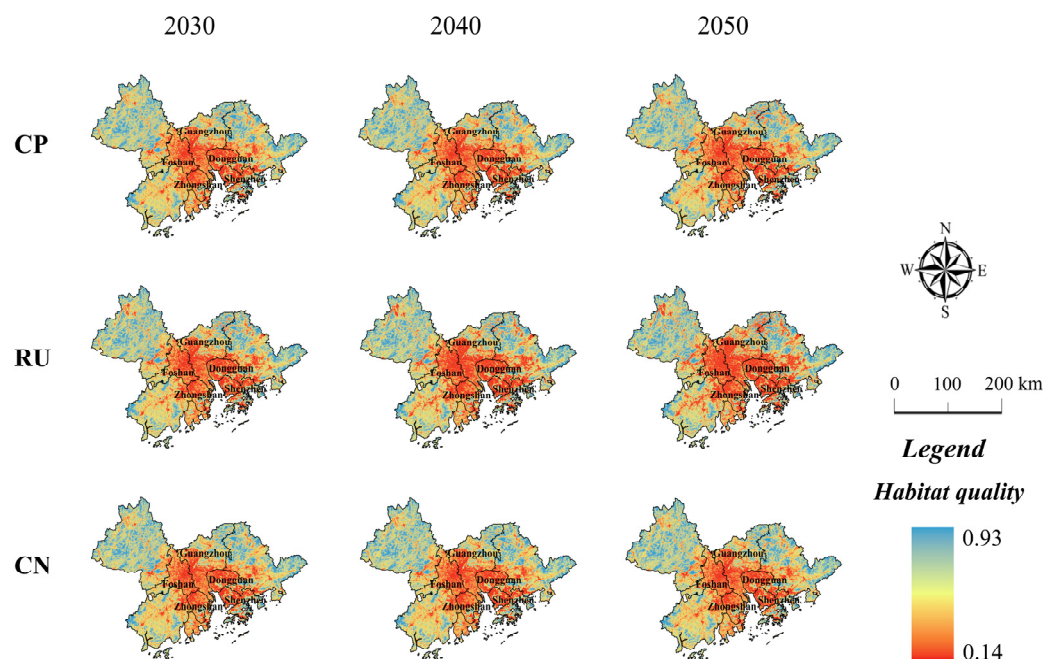


Figure 6. Dynamic habitat quality distributions for 2030, 2040 and 2050 under multi-scenarios. Note: CP, RU and CN refer to the cropland protection scenario, rapid urbanization scenario and carbon neutral scenario, respectively (unit: dimensionless parameter). Cities with lower habitat quality in GBA are marked.

3.4. Ecosystem Service Value Changes

The spatial distributions of ESVs exhibit similar changes with the habitat quality as a better ecological environment would gain higher ESVs generally (Figure 7). Overall, the ESVs of the GBA are expected to continuously decline from 2030 to 2050 under both the RU and CP scenarios. In the RU scenario, the northwestern and northeastern GBA have higher ESVs, including Zhaoqing, the northern Guangzhou and the northern Huizhou. In contrast, the central GBA shows relatively low ESVs, which are even below CNY 1123/pixel for the period 2020 to 2050 and less than half of the surrounding ESVs. The spatiotemporal characteristics and changing trends of ESVs in the CP scenario are similar to those in the RU scenario. However, the total ESVs in the CP scenario are slightly higher than that in the RU scenario. The CN scenario demonstrates an overall opposite trend, with ESVs increasing from 2030 to 2050 when compared to the other two scenarios. GBA in 2050 would own the highest ESVs distribution, particularly in the northwestern and northeastern GBA, where ESVs are greater than CNY 5210/pixel for the enclosing suburban areas. In the CN scenario, the ESVs in the central GBA are higher than those in the other two scenarios and keep rising from 2030 to 2050.

In detail, the values of second-level ES and the ESVs of each city are compared (Figure 8). The values of water regulation and climate regulation are high, indicating the high level of ecosystem adjustment between nature and anthropogenic activities. However, the values of raw materials, water supply and nutrient cycling maintenance are low, which implies a relatively low capability for providing production resources. Water supply is negative under three scenarios except for the RU scenario as the equivalent coefficient of water supply of cropland is negative and the area of cropland in the RU scenario is nearly 4000 km² less than that in the CP and CN scenarios. In each second-level ES, the ESVs of the CN scenario are commonly the highest, followed by the CP and RU scenarios. Compared with ESVs in 2020, the values of raw materials, water supply, gas regulation, climate

regulation, environment purification, soil conservation and nutrient cycling maintenance in the CN scenario are all higher, while only water supply in the CP and RU scenarios are higher than in 2020. In the statistics chart for each city, Zhaoqing, Huizhou, Jiangmen and Guangzhou have the highest ESVs among all GBA cities. Cities with faster economic development have lower ESVs, with Macao being the lowest. Furthermore, the ESVs of the CN scenario are the highest and the ESVs of the CP scenario are slightly higher than those of the RU scenario in each city, resulting from the variations in the total areas of different land use types.

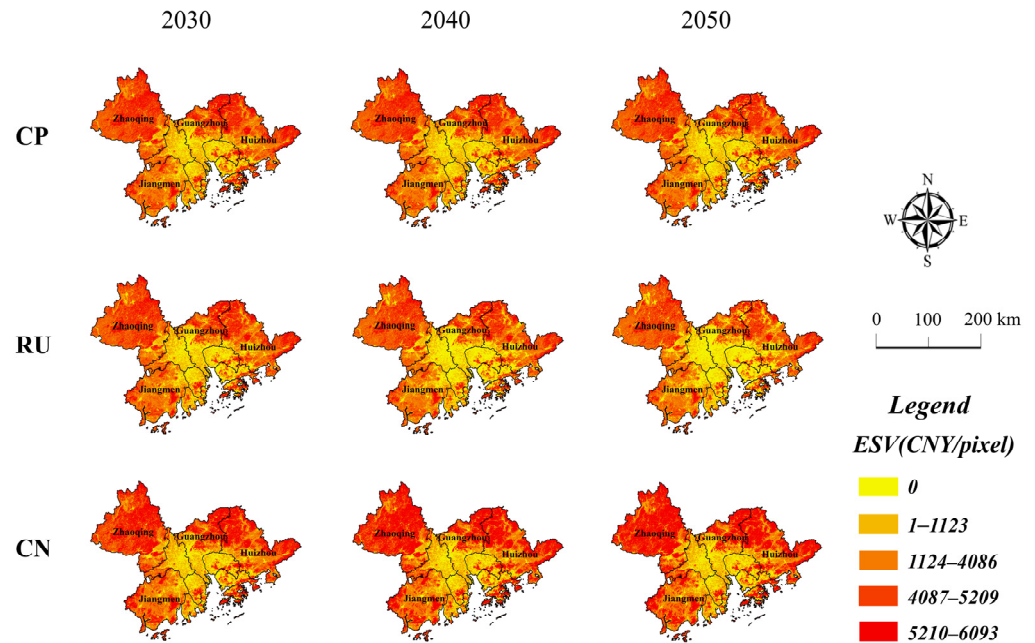


Figure 7. Dynamic ecosystem service value distributions for 2030, 2040 and 2050 under multi-scenarios. Note: CP, RU and CN refer to the cropland protection scenario, rapid urbanization scenario and carbon neutral scenario, respectively. Cities with higher ESV in GBA are marked.

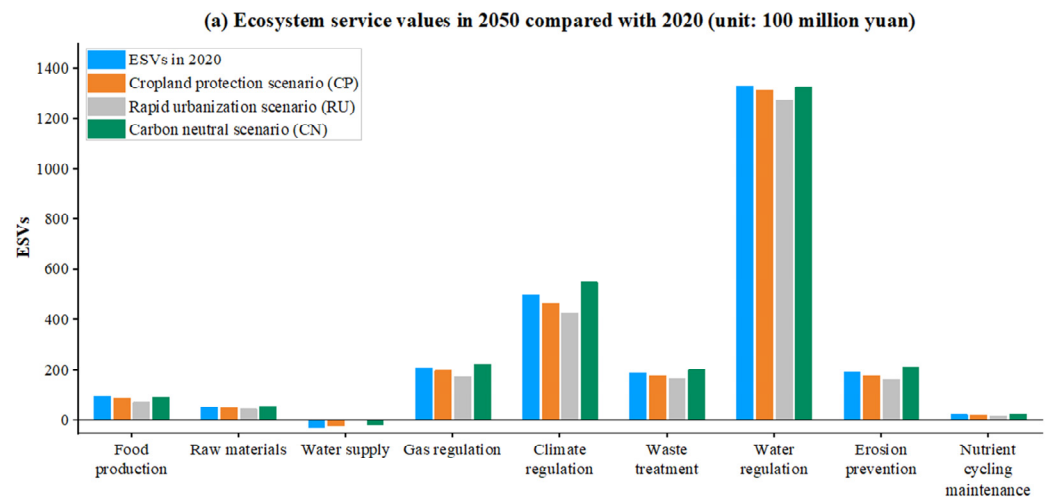


Figure 8. Cont.

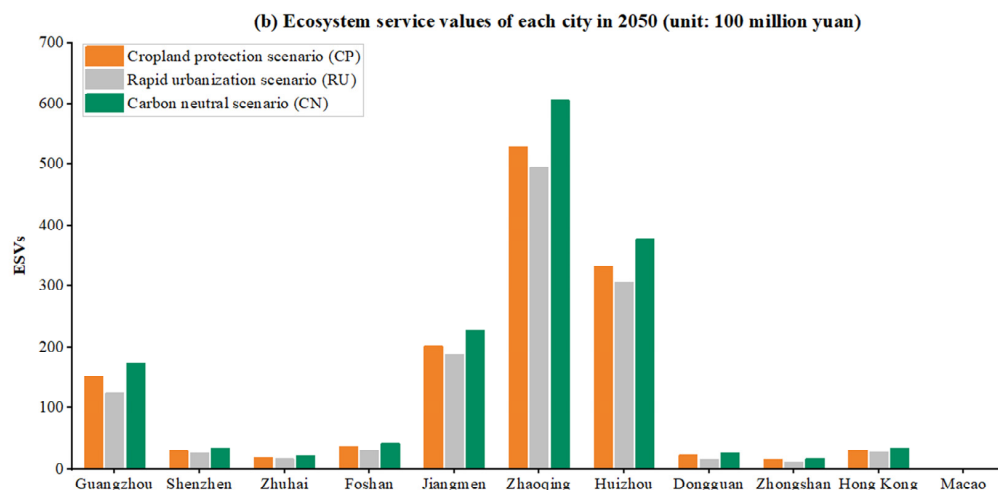


Figure 8. (a) Ecosystem service values in 2020 and in 2050 under CP, RU and CN scenarios (unit: CNY 100 million); (b) ecosystem service values of each city in the GBA in 2050 under CP, RU and CN scenarios (unit: CNY 100 million). Note: CP, RU and CN refer to the cropland protection scenario, rapid urbanization scenario and carbon neutral scenario, respectively.

3.5. Ecological Risk Assessment

The ecological risk values are classified into five levels (I to V) to quantitatively assess the ecological risk among three scenarios, as shown in Figure 9. The ecological risk exhibits similar characteristics among the three scenarios. In the RU scenario, the ecological risk is higher in the central and southwestern GBA while lower in the northwestern and northeastern GBA. The percentage of level I in the RU scenario is lower than that in the CP and CN scenarios, falling about 4%. Notably, the total percentage of level IV and level V exceeds 25%. In the CP scenario, the spatial distribution of ecological risk is similar to that in the RU scenario. However, the overall ecological risk in the CP scenario is lower than that in the RU scenario. The percentage of level I is 36.0%, which is higher than that in the RU scenario. Moreover, the total percentage of level IV and level V is lower than that in the RU scenario, which is less than 25%. In the CN scenario, the spatial distribution of ecological risk bears resemblance to that in the CP and RU scenarios. Nevertheless, the overall ecological risk in the CN scenario is lower than that in the CP and RU scenarios. The total percentage of level I and level II in the CN scenario reaches 58.5%, whereas it is lower than 30% in the CP scenario. Additionally, the total percentage of level IV and level V in the CN scenario is approximately 6% lower than that in the RU scenario. Overall, the CN scenario exhibits the lowest ecological risk among the three scenarios.

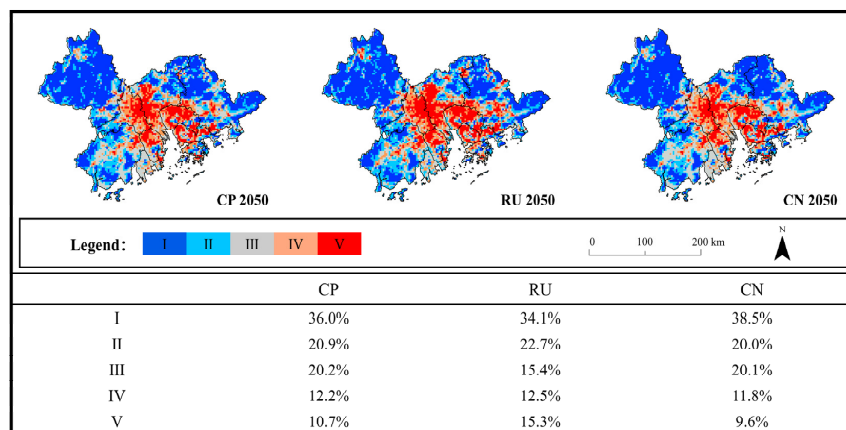


Figure 9. Dynamic ecological risk distributions for 2050 under multi-scenarios. Note: CP, RU and CN refer to the cropland protection scenario, rapid urbanization scenario and carbon neutral scenario, respectively.

3.6. Impact of Land Use on ESV Changes

Figure 10 shows the ESV flows from 2020 to 2050 for each land use type under multi-scenarios. In the CP and RU scenarios, the ESVs of cropland and forest decrease while those of grassland and shrubland increase during the period of 2020–2050. Both RU and CP scenarios experience the largest reduction in the ESVs of forest, with a decrease of up to more than CNY 28 billion and more than CNY 11 billion, respectively. The ESV flows transforming to urban in the RU scenario are also higher than in the CP scenario. However, the ESVs of forest in the CN scenario significantly increase, and the increment exceeds CNY 36 billion from 2020 to 2050. The ESV flows transforming to urban in the CN scenario are far less than those in the RU scenario. Nevertheless, the ESVs of cropland, grassland and shrubland all decrease, with the ESVs of shrubland decreasing the most, and the ESV flows mainly concentrate in shrubland and forest, which are larger than those in the CP and RU scenarios. The “other” land use type, primarily composed of water bodies, owns high ESVs which remain constant between 2020 and 2050 among three scenarios.

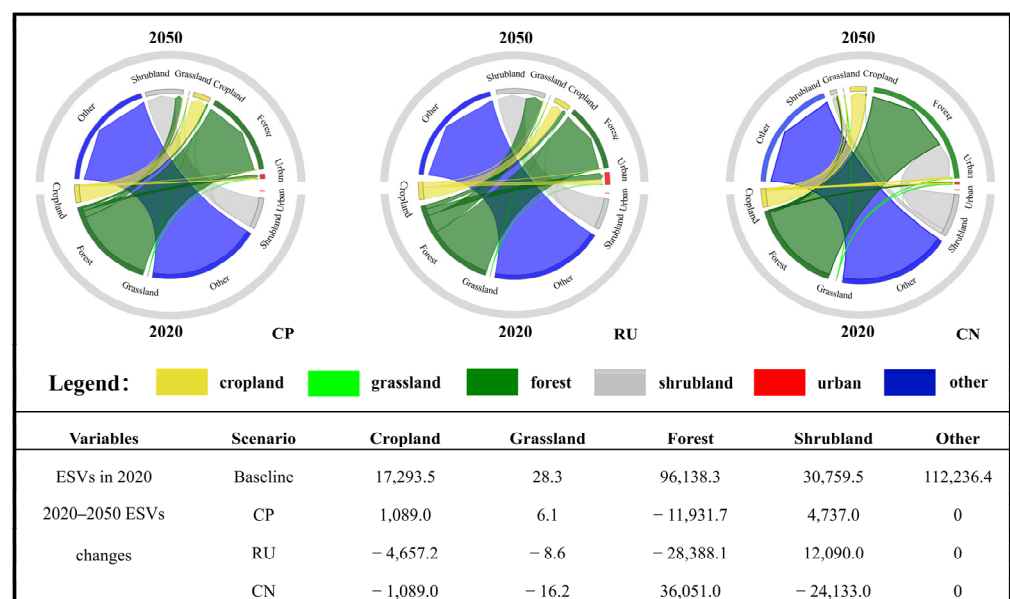


Figure 10. The ESV flows from 2020 to 2050 for each land use type (unit: CNY million). Note: CP, RU and CN refer to the cropland protection scenario, rapid urbanization scenario and carbon neutral scenario, respectively.

The spatial clustering of ESVs indicates a center cold clustering surrounded by hot spots clustering distribution (Figure 11). In the RU and CP scenarios, the hot-spot areas are mainly concentrated in Zhaoqing, located in the northwestern GBA. Several small hot-spot areas exist in Huizhou and Jiangmen, which are in the northeastern and southwestern GBA, respectively. The hot spot confidence reaches 99%. Cold-spot areas are concentrated in the central GBA, including Guangzhou, Foshan, Dongguan and Zhongshan, where the cold-spot confidence ranges from 90% to 99%. Compared with the CP scenario, the RU scenario exhibits lower spatial clustering of hot-spot areas in the northwestern GBA, but higher spatial cold-spot clustering in the central GBA. In the CN scenario, the spatial clustering of ESVs is the lowest among the three scenarios. Large areas in the southwest, northeast, and even part of northwest regions are the regions with low significance levels. In contrast to the spatial distribution of ESVs hot/cold spots in 2020, both the RU and CP scenarios show that the spatial clustering of the hot-spot areas is stronger in the northwestern GBA while weaker in the northeastern GBA, and the cold-spot areas in the central GBA slightly expand from the center to the surrounding region. The spatial clustering trends of the CN scenario seem to be more scattered in both the center and surrounding regions, with the significance level becoming lower than that in 2020.

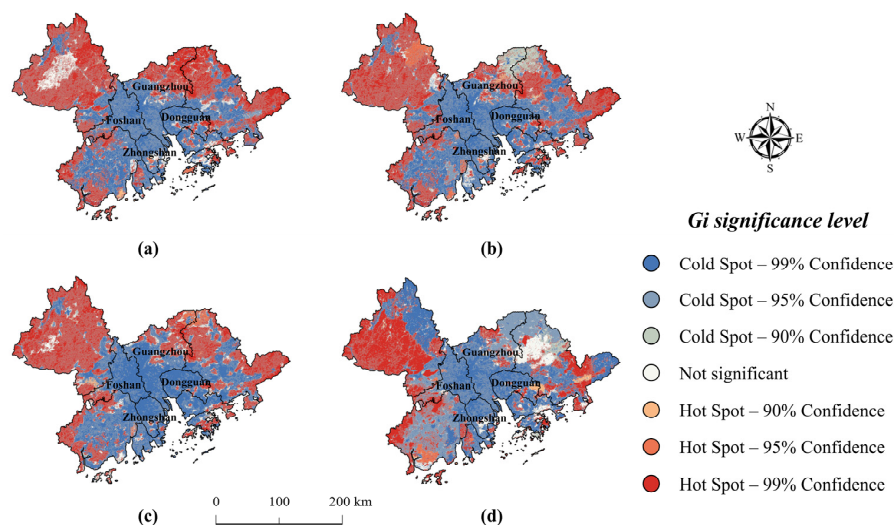


Figure 11. (a) Spatial distribution of ecosystem service values (ESVs) hot/cold spots in 2020. (b) Spatial distribution of ESVs hot/cold spots under cropland protection (CP) scenario in 2050. (c) Spatial distribution of ESVs hot/cold spots under rapid urbanization (RU) scenario in 2050. (d) Spatial distribution of ESVs hot/cold spots under carbon neutral (CN) scenario in 2050.

4. Discussion

4.1. Land Use Change Impact on ES and ESVs

The LUCC has a close connection with carbon storage and habitat quality [56,57], in which forest is a crucial factor for carbon storage capability [58], while urban areas could strongly damage habitat quality [59]. Among the six land use types, the carbon storage from highest to lowest is forest, grassland, cropland, shrubland, “other” and urban. It is worth noting that forests and grassland have higher carbon storage than other land use types. Consequently, the larger the green space area, the higher the carbon storage. The total carbon storage of the CN scenario is higher than that in the CP and RU scenarios as the vegetation area is significantly substantial, especially the forest area. Similar to carbon storage, the habitat quality of forest, grassland and shrubland ranks in the top three while urban areas are the lowest. Abundant vegetation is beneficial for improving habitat quality. Meanwhile, the LUCC exhibits significant spatiotemporal heterogeneity under three scenarios from 2030 to 2050 [60,61]. According to Xie et al. [21], different land use types have distinct equivalent coefficients in each second-level ES. Among these land use types, the sum of equivalent coefficients of “other” is the highest as the equivalent coefficient of hydrological regulation of “other” is remarkably higher than that of other second-level ES. However, “other” is set as a constraint layer, which is prohibited from transforming into any land use type, resulting in the ESV change of “other” from 2030 to 2050 as 0. Beyond that, the order of ESV contribution rates from high to low are forest, grassland, shrubland and cropland, which is consistent with those of Liang and Song [62]. The results show that the LUCC would dominate the spatial-temporal changes of ESVs.

4.2. The Relationship between Ecological Risk and LUCC

As shown in Table 3, the weights of the proportion of built-up land are the highest, followed by the land-use composite index, ecological capacity and ESV. Based on our research, it can be inferred that these indicators are closely associated with LUCC. In the RU scenario, urban expands extensively, encroaching upon vast forest and cropland, consequently resulting in the increase of built-up land area and the decline of ESVs and EC, so the ecological risk remains at a high level. In contrast, the CP scenario exhibits a smaller urban area, while the areas of cropland and forest are larger than those in the RU scenario. As a result, the ESVs are higher in the CP scenario. In addition, the expansion of forest area contributes to the enhancement of carbon storage and habitat quality, thereby improving

EC and subsequently mitigating ecological risk. In the CN scenario, the urban area is far less than that in the other two scenarios, while the forest area largely increases, leading to the lowest ecological risk. In general, LUCC exerts a profound impact on ecological risk. Urban expansion usually leads to the degradation of the ecological environment and an increase in ecological risk. Conversely, forests and cropland contribute to improving the environmental quality and reducing ecological risk.

4.3. Land Use Strategies under Multiple Scenarios

Based on different land use strategies, LUCC development in three scenarios exhibits unique characteristics, ultimately influencing ES, ESVs and ecological risk. The RU scenario can promote rapid urban expansion, but it causes significant damage to the ecological environment and the ecological risk is remarkably elevated. Compared with the RU scenario, the CP scenario can protect the cropland and forest more effectively. Its contribution to carbon storage, habitat quality and ESVs is relatively larger. The CN scenario imposes strict limitations on urban development and attaches more importance to forest protection, so ES and ESVs in the CN scenario remain at the highest level and the ecological risk is the lowest among the three scenarios. Therefore, based on the CN scenario, a balanced approach is required that incorporates forest conservation and urban development [63–65]. In the future, we should strike a balance between urban expansion and ecological protection. Neither should we go all out for economic development at the expense of ecological protection, nor should we simply protect the ecological environment at the expense of the economy. More protection should be given to forests and cropland in the future as they possess great ecological value. In the meantime, land-use policies should be formulated in line with the ecological characteristics of different regions [66]. The unorganized urban expansion should be limited and the ecological spatial patterns need to be further constructed in the central GBA [67,68]. Meanwhile, the ecosystem structure ought to be stabilized in the northwestern, northeastern and southwestern GBA, as usual [46].

5. Conclusions

In this study, we simulate the future LUCC and evaluate ES, ESV changes and the induced ecological risk in 2030, 2040 and 2050 under three scenarios. The relationships between LUCC and these ecological indicators are also evaluated. The results are as follows:

- (1) The spatiotemporal heterogeneity of land-use patterns under different scenarios is significant. The RU scenario shows extremely high urban expansion in the central GBA at the expense of cropland and forest, which does not align with sustainable development goals. The CP scenario focuses on cropland protection. In contrast, the CN scenario has a conspicuous increase in forest area and an effective limitation in urban expansion, which is in line with the sustainable development goal.
- (2) Owing to the high rate of urban expansion, carbon storage and habitat quality are lower in the CP and RU scenarios, whereas they are higher in the CN scenario. The ESVs in the CP and RU scenarios are lower than in the CN scenario. The cold and hot spots of ESVs show aggregated distributions except for the CN scenario.
- (3) The ecological risk is closely linked to LUCC, which exhibits a higher trend in the central and southwestern GBA and lower in the northwestern and northeastern GBA. Among the three scenarios, the RU poses the highest ecological risk while the CN owns the lowest ecological risk, in which ESVs and EC rank are the top two factors, indicating a close association between LUCC and ecological risk.
- (4) In order to achieve carbon peaking and carbon neutrality goals, the government should formulate specific policies based on the different land-use conditions. In the central GBA, rationalizing urban expansion and strengthening the protection of ecological resources should be important tasks. In the northwestern, northeastern and southwestern GBA, it is advisable to highlight ecological carbon sequestration measures.

However, there are several limitations in this research. Due to the data of grain production value and the sown area in the future being difficult to predict, a constant standard unit

equivalent factor per unit area is used in ESV calculation. Dynamic standard unit equivalent factors are needed in the future to achieve more accurate estimation. Additionally, the habitat suitability of each land use type is determined by expert knowledge [44], which possesses a certain degree of subjectivity and should be further improved by considering the systematic impacts of different threats on habitat quality. In the assessment of ecological risk, the entropy method used to determine the weights of indicators is sensitive to the sample data and lack of dynamic variation. Therefore, it is better to integrate with expert knowledge so as to determine the weights more scientifically.

Supplementary Materials: The following supporting information can be downloaded at: <https://www.mdpi.com/article/10.3390/rs15245749/s1>, Figure S1: (a) land cover map of 2000; (b) land cover map of 2010. Figure S2: maps of nine driving factors: (a) distance to railway; (b) distance to road; (c) distance to water; (d) soil type; (e) precipitation; (f) temperature; (g) population (h) GDP (i) DEM. Table S1: reclassification of land-use data from multiple models; Table S2: the information on driving factors.

Author Contributions: H.C.: writing—original draft and data curation. N.D.: writing—review and editing, conceptualization and methodology. X.L.: review, software and data curation. H.H.: review and data curation. All authors have read and agreed to the published version of the manuscript.

Funding: This research was supported by the National Natural Science Foundation of China (Grant No. 42301027), Basic and Applied Basic Research Foundation of Guangdong (Grant ID 2022A1515111033), and China Meteorological Administration climate change special project (Grant ID QBZ202313).

Data Availability Statement: The data presented in this paper are contained within the article and Supplementary Materials.

Conflicts of Interest: The authors declare no conflict of interest.

References

1. Guo, P.; Wang, H.; Qin, F.; Miao, C.; Zhang, F. Coupled MOP and PLUS-SA Model Research on Land Use Scenario Simulations in Zhengzhou Metropolitan Area, Central China. *Remote Sens.* **2023**, *15*, 3762. [[CrossRef](#)]
2. Zhang, X.; Ren, W.; Peng, H. Urban land use change simulation and spatial responses of ecosystem service value under multiple scenarios: A case study of Wuhan, China. *Ecol. Indic.* **2022**, *144*, 109526. [[CrossRef](#)]
3. Schirpke, U.; Tscholl, S.; Tasser, E. Spatio-temporal changes in ecosystem service values: Effects of land-use changes from past to future (1860–2100). *J. Environ. Manag.* **2020**, *272*, 111068. [[CrossRef](#)] [[PubMed](#)]
4. Verburg, P.H.; Soepboer, W.; Veldkamp, A.; Limpiada, R.; Espaldon, V.; Mastura, S.S. Modeling the spatial dynamics of regional land use: The CLUE-S model. *Environ. Manag.* **2002**, *30*, 391–405. [[CrossRef](#)] [[PubMed](#)]
5. Sohl, T.L.; Saylor, K.L.; Drummond, M.A.; Loveland, T.R. The FORE-SCE model: A practical approach for projecting land cover change using scenario-based modeling. *J. Land Use Sci.* **2007**, *2*, 103–126. [[CrossRef](#)]
6. Liang, X.; Guan, Q.; Clarke, K.C.; Liu, S.; Wang, B.; Yao, Y. Understanding the drivers of sustainable land expansion using a patch-generating land use simulation (PLUS) model: A case study in Wuhan, China. *Comput. Environ. Urban Syst.* **2021**, *85*, 101569. [[CrossRef](#)]
7. Gao, L.; Tao, F.; Liu, R.; Wang, Z.; Leng, H.; Zhou, T. Multi-scenario simulation and ecological risk analysis of land use based on the PLUS model: A case study of Nanjing. *Sustain. Cities Soc.* **2022**, *85*, 104055. [[CrossRef](#)]
8. Li, C.; Wu, Y.; Gao, B.; Zheng, K.; Wu, Y.; Li, C. Multi-scenario simulation of ecosystem service value for optimization of land use in the Sichuan-Yunnan ecological barrier, China. *Ecol. Indic.* **2021**, *132*, 108328. [[CrossRef](#)]
9. Grafius, D.R.; Corstanje, R.; Warren, P.H.; Evans, K.L.; Hancock, S.; Harris, J.A. The impact of land use/land cover scale on modelling urban ecosystem services. *Landsc. Ecol.* **2016**, *31*, 1509–1522. [[CrossRef](#)]
10. Li, P.; Chen, J.; Li, Y.; Wu, W. Using the InVEST-PLUS Model to Predict and Analyze the Pattern of Ecosystem Carbon storage in Liaoning Province, China. *Remote Sens.* **2023**, *15*, 4050. [[CrossRef](#)]
11. Li, Y.; Yao, S.; Jiang, H.; Wang, H.; Ran, Q.; Gao, X.; Ding, X.; Ge, D. Spatial-Temporal Evolution and Prediction of Carbon Storage: An Integrated Framework Based on the MOP-PLUS-InVEST Model and an Applied Case Study in Hangzhou, East China. *Land* **2022**, *11*, 2213. [[CrossRef](#)]
12. Ouyang, X.; Tang, L.; Wei, X.; Li, Y. Spatial interaction between urbanization and ecosystem services in Chinese urban agglomerations. *Land Use Policy* **2021**, *109*, 105587. [[CrossRef](#)]
13. Silvestri, S.; Zaibet, L.; Said, M.Y.; Kifugo, S.C. Valuing ecosystem services for conservation and development purposes: A case study from Kenya. *Environ. Sci. Policy* **2013**, *31*, 23–33. [[CrossRef](#)]

14. Sun, J.; Zhang, Y.; Qin, W.; Chai, G. Estimation and simulation of forest carbon stock in northeast China forestry based on future climate change and LUCC. *Remote Sens.* **2022**, *14*, 3653. [[CrossRef](#)]
15. Wang, Z.; Li, X.; Mao, Y.; Li, L.; Wang, X.; Lin, Q. Dynamic simulation of land use change and assessment of carbon storage based on climate change scenarios at the city level: A case study of Bortala, China. *Ecol. Indic.* **2022**, *134*, 108499. [[CrossRef](#)]
16. Yang, W.; Jin, Y.; Sun, T.; Yang, Z.; Cai, Y.; Yi, Y. Trade-offs among ecosystem services in coastal wetlands under the effects of reclamation activities. *Ecol. Indic.* **2018**, *92*, 354–366. [[CrossRef](#)]
17. Nelson, D.A. European Environment Agency. *Colo. J. Int. Environ. Law Policy* **1999**, *10*, 153.
18. Hu, M.; Li, Z.; Wang, Y.; Jiao, M.; Li, M.; Xia, B. Spatio-temporal changes in ecosystem service value in response to land-use/cover changes in the Pearl River Delta. *Resour. Conserv. Recycl.* **2019**, *149*, 106–114. [[CrossRef](#)]
19. Costanza, R.; d’Arge, R.; De Groot, R.; Farber, S.; Grasso, M.; Hannon, B.; Limburg, K.; Naeem, S.; O’neill, R.V.; Paruelo, J. The value of the world’s ecosystem services and natural capital. *Nature* **1997**, *387*, 253–260. [[CrossRef](#)]
20. Xie, G.-D.; Lu, C.X.; Leng, Y.-F.; Zheng, D.; Li, S.J. Ecological assets valuation of the Tibetan Plateau. *J. Nat. Resour.* **2003**, *18*, 189–196. [[CrossRef](#)]
21. Xie, G.; Zhang, C.; Zhen, L.; Zhang, L. Dynamic changes in the value of China’s ecosystem services. *Ecosyst. Serv.* **2017**, *26*, 146–154. [[CrossRef](#)]
22. Liu, W.; Zhan, J.; Zhao, F.; Yan, H.; Zhang, F.; Wei, X. Impacts of urbanization-induced land-use changes on ecosystem services: A case study of the Pearl River Delta Metropolitan Region, China. *Ecol. Indic.* **2019**, *98*, 228–238. [[CrossRef](#)]
23. Xie, Y.; Zhu, Q.; Bai, H.; Luo, P.; Liu, J. Spatio-Temporal Evolution and Coupled Coordination of LUCC and ESV in Cities of the Transition Zone, Shenmu City, China. *Remote Sens.* **2023**, *15*, 3136. [[CrossRef](#)]
24. Zhang, S.; Wang, Y.; Xu, W.; Sheng, Z.; Zhu, Z.; Hou, Y. Analysis of Spatial and Temporal Variability of Ecosystem Service Values and Their Spatial Correlation in Xinjiang, China. *Remote Sens.* **2023**, *15*, 4861. [[CrossRef](#)]
25. Jiang, X.; Zhai, S.; Liu, H.; Chen, J.; Zhu, Y.; Wang, Z. Multi-scenario simulation of production-living-ecological space and ecological effects based on shared socioeconomic pathways in Zhengzhou, China. *Ecol. Indic.* **2022**, *137*, 108750. [[CrossRef](#)]
26. Peng, K.; Jiang, W.; Ling, Z.; Hou, P.; Deng, Y. Evaluating the potential impacts of land use changes on ecosystem service value under multiple scenarios in support of SDG reporting: A case study of the Wuhan urban agglomeration. *J. Clean. Prod.* **2021**, *307*, 127321. [[CrossRef](#)]
27. Jin, X.; Jin, Y.; Mao, X. Ecological risk assessment of cities on the Tibetan Plateau based on land use/land cover changes—Case study of Delingha City. *Ecol. Indic.* **2019**, *101*, 185–191. [[CrossRef](#)]
28. Xu, Q.; Guo, P.; Jin, M.; Qi, J. Multi-scenario landscape ecological risk assessment based on Markov–FLUS composite model. *Geomat. Nat. Hazards Risk* **2021**, *12*, 1449–1466. [[CrossRef](#)]
29. Zhang, S.; Zhong, Q.; Cheng, D.; Xu, C.; Chang, Y.; Lin, Y.; Li, B. Landscape ecological risk projection based on the PLUS model under the localized shared socioeconomic pathways in the Fujian Delta region. *Ecol. Indic.* **2022**, *136*, 108642. [[CrossRef](#)]
30. Lin, Y.; Hu, X.; Zheng, X.; Hou, X.; Zhang, Z.; Zhou, X.; Qiu, R.; Lin, J. Spatial variations in the relationships between road network and landscape ecological risks in the highest forest coverage region of China. *Ecol. Indic.* **2019**, *96*, 392–403. [[CrossRef](#)]
31. Wu, J. Landscape sustainability science: Ecosystem services and human well-being in changing landscapes. *Landsc. Ecol.* **2013**, *28*, 999–1023. [[CrossRef](#)]
32. Gong, J.; Yang, J.; Tang, W. Spatially explicit landscape-level ecological risks induced by land use and land cover change in a national ecologically representative region in China. *Int. J. Environ. Res. Public Health* **2015**, *12*, 14192–14215. [[CrossRef](#)] [[PubMed](#)]
33. Jiang, M.; Chen, H.; Chen, Q. A method to analyze “source–sink” structure of non-point source pollution based on remote sensing technology. *Environ. Pollut.* **2013**, *182*, 135–140. [[CrossRef](#)] [[PubMed](#)]
34. Liu, Y.; Liu, Y.; Li, J.; Lu, W.; Wei, X.; Sun, C. Evolution of landscape ecological risk at the optimal scale: A case study of the open coastal wetlands in Jiangsu, China. *Int. J. Environ. Res. Public Health* **2018**, *15*, 1691. [[CrossRef](#)] [[PubMed](#)]
35. Yan, Z.; Wang, Y.; Wang, Z.; Zhang, C.; Wang, Y.; Li, Y. Spatiotemporal Analysis of Landscape Ecological Risk and Driving Factors: A Case Study in the Three Gorges Reservoir Area, China. *Remote Sens.* **2023**, *15*, 4884. [[CrossRef](#)]
36. Cui, L.; Zhao, Y.; Liu, J.; Han, L.; Ao, Y.; Yin, S. Landscape ecological risk assessment in Qinling Mountain. *Geol. J.* **2018**, *53*, 342–351. [[CrossRef](#)]
37. Li, W.; Wang, Y.; Xie, S.; Sun, R.; Cheng, X. Impacts of landscape multifunctionality change on landscape ecological risk in a megacity, China: A case study of Beijing. *Ecol. Indic.* **2020**, *117*, 106681. [[CrossRef](#)]
38. Wang, B.; Ding, M.; Li, S.; Liu, L.; Ai, J. Assessment of landscape ecological risk for a cross-border basin: A case study of the Koshi River Basin, central Himalayas. *Ecol. Indic.* **2020**, *117*, 106621. [[CrossRef](#)]
39. Xu, W.; Wang, J.; Zhang, M.; Li, S. Construction of landscape ecological network based on landscape ecological risk assessment in a large-scale opencast coal mine area. *J. Clean. Prod.* **2021**, *286*, 125523. [[CrossRef](#)]
40. Venkatesh, K.; John, R.; Chen, J.; Xiao, J.; Amirkhiz, R.G.; Giannico, V.; Kussainova, M. Optimal ranges of social-environmental drivers and their impacts on vegetation dynamics in Kazakhstan. *Sci. Total Environ.* **2022**, *847*, 157562. [[CrossRef](#)]
41. Zheng, K.; Tan, L.; Sun, Y.; Wu, Y.; Duan, Z.; Xu, Y.; Gao, C. Impacts of climate change and anthropogenic activities on vegetation change: Evidence from typical areas in China. *Ecol. Indic.* **2021**, *126*, 107648. [[CrossRef](#)]
42. Zhang, X.; Liu, L.; Chen, X.; Gao, Y.; Xie, S.; Mi, J. GLC_FCS30: Global land-cover product with fine classification system at 30 m using time-series Landsat imagery. *Earth Syst. Sci. Data* **2021**, *13*, 2753–2776. [[CrossRef](#)]

43. Wu, P.; Liu, X.; Li, X.; Chen, Y. Impact of urban expansion on carbon storage in terrestrial ecosystems based on InVEST model and CA: A case study of Guangdong Province. *Geogr. Geo-Inf. Sci.* **2016**, *32*, 22–28. [[CrossRef](#)]
44. Terrado, M.; Sabater, S.; Chaplin-Kramer, B.; Mandle, L.; Ziv, G.; Acuña, V. Model development for the assessment of terrestrial and aquatic habitat quality in conservation planning. *Sci. Total Environ.* **2016**, *540*, 63–70. [[CrossRef](#)] [[PubMed](#)]
45. Huang, Y.; Sun, W.; Qin, Z.; Zhang, W.; Yu, Y.; Li, T.; Zhang, Q.; Wang, G.; Yu, L.; Wang, Y. The role of China's terrestrial carbon sequestration 2010–2060 in offsetting energy-related CO₂ emissions. *Natl. Sci. Rev.* **2022**, *9*, nwac057. [[CrossRef](#)] [[PubMed](#)]
46. Andersson, E.; Langemeyer, J.; Borgstrom, S.; McPhearson, T.; Haase, D.; Kronenberg, J.; Barton, D.N.; Davis, M.; Naumann, S.; Roschel, L.; et al. Enabling Green and Blue Infrastructure to Improve Contributions to Human Well-Being and Equity in Urban Systems. *Bioscience* **2019**, *69*, 566–574. [[CrossRef](#)] [[PubMed](#)]
47. Nelson, E.; Mendoza, G.; Regetz, J.; Polasky, S.; Tallis, H.; Cameron, D.; Chan, K.M.; Daily, G.C.; Goldstein, J.; Kareiva, P.M. Modeling multiple ecosystem services, biodiversity conservation, commodity production, and tradeoffs at landscape scales. *Front. Ecol. Environ.* **2009**, *7*, 4–11. [[CrossRef](#)]
48. Xie, G.; Zhang, C.-X.; Zhang, L.-M.; Chen, W.; Li, S. Improvement of the evaluation method for ecosystem service value based on per unit area. *J. Nat. Resour.* **2015**, *30*, 1243. [[CrossRef](#)]
49. Ge, G.; Zhang, J.; Chen, X.; Liu, X.; Hao, Y.; Yang, X.; Kwon, S. Effects of land use and land cover change on ecosystem services in an arid desert-oasis ecotone along the Yellow River of China. *Ecol. Eng.* **2022**, *176*, 106512. [[CrossRef](#)]
50. Zhao, Q.; Wen, Z.; Chen, S.; Ding, S.; Zhang, M. Quantifying land use/land cover and landscape pattern changes and impacts on ecosystem services. *Int. J. Environ. Res. Public Health* **2020**, *17*, 126. [[CrossRef](#)]
51. Li, G.; Fang, C.; Wang, S. Exploring spatiotemporal changes in ecosystem-service values and hotspots in China. *Sci. Total Environ.* **2016**, *545*, 609–620. [[CrossRef](#)] [[PubMed](#)]
52. Su, L.; Fan, J.; Fu, L. Exploration of smart city construction under new urbanization: A case study of Jinzhou-Huludao Coastal Area. *Sustain. Comput. Inform. Syst.* **2020**, *27*, 100403. [[CrossRef](#)]
53. Han, Z.; Li, J.; Yin, H.; Shen, T.Y.J.; Xu, C. Analysis of ecological security of wetland in Liaohe River delta based on the landscape pattern. *Ecol. Environ. Sci.* **2010**, *19*, 701–705.
54. Guo, H.; Dong, S.; Wu, D.; Pei, S.; Xin, X. Calculation and analysis of equivalence factor and yield factor of ecological footprint based on ecosystem services value. *Acta Ecol. Sin.* **2020**, *40*, 1405–1412. [[CrossRef](#)]
55. Zou, Z.-H.; Yi, Y.; Sun, J.-N. Entropy method for determination of weight of evaluating indicators in fuzzy synthetic evaluation for water quality assessment. *J. Environ. Sci.* **2006**, *18*, 1020–1023. [[CrossRef](#)] [[PubMed](#)]
56. Li, Y.; Liu, W.; Feng, Q.; Zhu, M.; Yang, L.; Zhang, J.; Yin, X. The role of land use change in affecting ecosystem services and the ecological security pattern of the Hexi Regions, Northwest China. *Sci. Total Environ.* **2023**, *855*, 158940. [[CrossRef](#)] [[PubMed](#)]
57. Zhu, G.; Qiu, D.; Zhang, Z.; Sang, L.; Liu, Y.; Wang, L.; Zhao, K.; Ma, H.; Xu, Y.; Wan, Q. Land-use changes lead to a decrease in carbon storage in arid region, China. *Ecol. Indic.* **2021**, *127*, 107770. [[CrossRef](#)]
58. Fahey, T.J.; Woodbury, P.B.; Battles, J.J.; Goodale, C.L.; Hamburg, S.P.; Ollinger, S.V.; Woodall, C.W. Forest carbon storage: Ecology, management, and policy. *Front. Ecol. Environ.* **2010**, *8*, 245–252. [[CrossRef](#)]
59. Song, Y.; Chen, B.; Kwan, M.-P. How does urban expansion impact people's exposure to green environments? A comparative study of 290 Chinese cities. *J. Clean. Prod.* **2020**, *246*, 119018. [[CrossRef](#)]
60. Fan, F.; Xiao, C.; Feng, Z.; Chen, Y. Land-planning management based on multiple ecosystem services and simulation in tropical forests. *J. Environ. Manag.* **2022**, *323*, 116216. [[CrossRef](#)]
61. Huang, A.; Xu, Y.; Sun, P.; Zhou, G.; Liu, C.; Lu, L.; Xiang, Y.; Wang, H. Land use/land cover changes and its impact on ecosystem services in ecologically fragile zone: A case study of Zhangjiakou City, Hebei Province, China. *Ecol. Indic.* **2019**, *104*, 604–614. [[CrossRef](#)]
62. Liang, Y.; Song, W. Integrating potential ecosystem services losses into ecological risk assessment of land use changes: A case study on the Qinghai-Tibet Plateau. *J. Environ. Manag.* **2022**, *318*, 115607. [[CrossRef](#)] [[PubMed](#)]
63. Li, J.; Guo, X.; Chuai, X.; Xie, F.; Yang, F.; Gao, R.; Ji, X. Reexamine China's terrestrial ecosystem carbon balance under land use-type and climate change. *Land Use Policy* **2021**, *102*, 105275. [[CrossRef](#)]
64. Li, J.; Ouyang, X.; Zhu, X. Land space simulation of urban agglomerations from the perspective of the symbiosis of urban development and ecological protection: A case study of Changsha-Zhuzhou-Xiangtan urban agglomeration. *Ecol. Indic.* **2021**, *126*, 107669. [[CrossRef](#)]
65. Li, M.; Liang, D.; Xia, J.; Song, J.; Cheng, D.; Wu, J.; Cao, Y.; Sun, H.; Li, Q. Evaluation of water conservation function of Danjiang River Basin in Qinling Mountains, China based on InVEST model. *J. Environ. Manag.* **2021**, *286*, 112212. [[CrossRef](#)] [[PubMed](#)]
66. Cao, Y.; Kong, L.; Zhang, L.; Ouyang, Z. The balance between economic development and ecosystem service value in the process of land urbanization: A case study of China's land urbanization from 2000 to 2015. *Land Use Policy* **2021**, *108*, 105536. [[CrossRef](#)]
67. Fang, Z.; Ding, T.; Chen, J.; Xue, S.; Zhou, Q.; Wang, Y.; Wang, Y.; Huang, Z.; Yang, S. Impacts of land use/land cover changes on ecosystem services in ecologically fragile regions. *Sci. Total Environ.* **2022**, *831*, 154967. [[CrossRef](#)] [[PubMed](#)]
68. Ma, Q. Integrating ecological correlation into cellular automata for urban growth simulation: A case study of Hangzhou, China. *Urban For. Urban Green.* **2020**, *51*, 126697. [[CrossRef](#)]

Disclaimer/Publisher's Note: The statements, opinions and data contained in all publications are solely those of the individual author(s) and contributor(s) and not of MDPI and/or the editor(s). MDPI and/or the editor(s) disclaim responsibility for any injury to people or property resulting from any ideas, methods, instructions or products referred to in the content.